



Cite this: *Analyst*, 2017, **142**, 2104

Received 17th March 2017,  
 Accepted 5th May 2017

DOI: 10.1039/c7an00467b

rsc.li/analyst

## An arylboronate locked fluorescent probe for hypochlorite†

Leilei Shi,<sup>‡a</sup> Xin Li,<sup>‡b</sup> Min Zhou,<sup>a</sup> Faheem Muhammad,<sup>a</sup> Yubin Ding<sup>id</sup> <sup>\*a,c</sup> and Hui Wei<sup>id</sup> <sup>\*a</sup>

An unusual arylboronate based fluorescent probe **R1** was synthesized for the selective and sensitive detection of  $\text{ClO}^-$ . A detailed mechanistic study revealed that **R1** reacted with  $\text{ClO}^-$  through an oxidation to chlorination mechanism, and the arylboronate moiety in **R1** acted as a “lock” to eliminate the effects of pH fluctuations. With this design strategy, **R1** was successfully used to detect as low as 6.4 nM of  $\text{ClO}^-$  over other ROS species in a wide pH range from 4.5 to 9.0.

### Introduction

Reactive oxygen species (ROS) (such as hydrogen peroxide, superoxide radical, singlet oxygen, hydroxyl radical, and hypochlorite anion) play critical roles in biological functions like cell signaling and homeostasis. A high level of ROS would lead to oxidative stress conditions, the damaging effects of which are the contributing factors of many diseases.<sup>1</sup> Among them, the hypochlorite anion ( $\text{ClO}^-$ ) has attracted particular attention due to its importance in immune systems against microorganisms and inflammation.<sup>2</sup> The dysregulated production of  $\text{ClO}^-$  in living systems may cause severe adverse effects and even diseases (such as cardiovascular diseases,<sup>3</sup> nephropathy,<sup>4</sup> neurodegenerative diseases,<sup>5</sup> and cancers<sup>6</sup>). Thus, the development of effective detection methods for monitoring  $\text{ClO}^-$  levels in living systems is of great importance.

Organic molecule based fluorescent probes have been demonstrated to be ideal tools for detecting various kinds of analytes such as metal ions, anions, small molecules, and bio-macromolecules.<sup>7</sup> Recently, numerous fluorescent probes have been successfully developed for  $\text{ClO}^-$  detection. Compared to other methods using chemiluminescent,<sup>8</sup> colourimetric,<sup>9</sup> or electrochemical<sup>10</sup> probes, these fluorescent probe based methods have advantages including low cost, easy fabrication, and high sensitivity. However, the selective recognition of  $\text{ClO}^-$  from the other coexisting ROS species with a fluorescent probe is still a challenging task.<sup>11</sup> Particularly, it is important to differentiate  $\text{ClO}^-$  from  $\text{H}_2\text{O}_2$  because  $\text{ClO}^-$  is endogenously produced by the myeloperoxidase (MPO) catalyzed reaction of  $\text{H}_2\text{O}_2$  and  $\text{Cl}^-$ .

Conventionally, arylboronate based fluorescent probes have been designed for the selective detection of  $\text{H}_2\text{O}_2$ .<sup>12</sup> However, one recent report showed that arylboronate could react faster with  $\text{ClO}^-$  than with  $\text{H}_2\text{O}_2$ .<sup>13</sup> Yoon *et al.* have exploited this phenomenon to develop a specific fluorescent probe containing both arylboronate and thiolactone moieties for  $\text{ClO}^-$  detection.<sup>11e</sup> They showed that among the ROS tested only  $\text{ClO}^-$  reacted with the arylboronate and then hydrolyzed the thiolactone moieties to generate detectable fluorescence signals. This example indicated that the arylboronate group may be developed as a powerful recognition unit to distinguish  $\text{ClO}^-$  from  $\text{H}_2\text{O}_2$ , as it may react with both  $\text{ClO}^-$  and  $\text{H}_2\text{O}_2$  but give different final products. However, selective and sensitive arylboronate based fluorescent probes for  $\text{ClO}^-$  are still very rare.

Moreover, an ideal fluorescent probe for living systems should also be robust to environmental fluctuations such as pH changes, because the pH values of the extracellular matrix, intracellular environment, and subcellular organelles are all different. We envisioned that one strategy to address this problem is to introduce a “locked” moiety in the detection system, which would only be removed at the site of interest. With these thoughts in mind, we herein report a fluorescent probe **R1**, in the structure of which the arylboronate group functions as both the  $\text{ClO}^-$  recognition unit and the “lock” to eliminate the effects of pH fluctuations (Scheme 1). The reac-

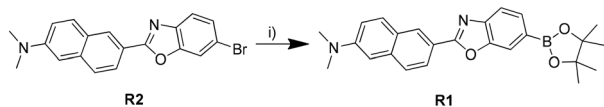
<sup>a</sup>Department of Biomedical Engineering, College of Engineering and Applied Sciences, Collaborative Innovation Center of Chemistry for Life Sciences, Nanjing National Laboratory of Microstructures, Nanjing University, Nanjing, Jiangsu 210093, China. E-mail: weihui@nju.edu.cn, ybding@njau.edu.cn; <http://www.weilab.nju.edu.cn>; Fax: +86-25-83594648; Tel: +86-25-83593272

<sup>b</sup>Division of Theoretical Chemistry and Biology, School of Biotechnology, KTH Royal Institute of Technology, SE-10691 Stockholm, Sweden

<sup>c</sup>Jiangsu Key Laboratory of Pesticide Science, College of Sciences, Nanjing Agricultural University, Nanjing, Jiangsu 210095, China

† Electronic supplementary information (ESI) available: Experimental details and additional figures. See DOI: 10.1039/c7an00467b

‡ These authors contributed equally.



**Scheme 1** Synthesis of fluorescent probe **R1**. (i) Bis(pinacolato)diboron,  $\text{CH}_3\text{COOK}$ ,  $\text{Pd}(\text{dppf})\text{Cl}_2$ , 1,4-dioxane, reflux.

tion mechanisms between **R1** and  $\text{ClO}^-$  and  $\text{H}_2\text{O}_2$  were investigated in detail. We found that compared with the unlocked molecule **R1-OH**, **R1** worked well in a much wider pH range from 4.5 to 9.0. Besides, probe **R1** was determined to be quite stable, and it was successfully used to selectively detect as low as 6.4 nM of  $\text{ClO}^-$  over other ROS species in a ratiometric way.

## Results and discussion

Probe **R1** was synthesized by the Miyaura borylation of the bromide precursor **R2** in a yield of 87% and characterized by NMR and mass spectrometry (MS) (Scheme 1 and Fig. S1–S3†). **R1** was stable and can be stored at room temperature for several weeks without obvious decomposition. When excited at 370 nm, **R1** emitted a strong blue/cyan fluorescence with a peak centered at  $\sim 481$  nm.

The reactivity and selectivity of **R1** toward  $\text{ClO}^-$  detection was then accessed in comparison to other ROS species. To our surprise, the addition of excess  $\text{H}_2\text{O}_2$  into **R1** solution did not induce significant fluorescence changes. Instead, among various tested ROS (such as  $^1\text{O}_2$ ,  $\text{O}_2^{\cdot-}$ ,  $\text{NO}^\cdot$ ,  $\text{ROO}^\cdot$ ,  $\text{HO}^\cdot$ ,  $\text{H}_2\text{O}_2$ ,  $\text{ONOO}^-$ , and  $\text{ClO}^-$ ), only the addition of  $\text{ClO}^-$  to **R1** solution resulted in a vivid emission colour change from blue/cyan to yellow under UV irradiation (Fig. 1a, inset). More surprisingly, we found that the reaction between **R1** and  $\text{H}_2\text{O}_2$  in EtOH resulted in a clear new product point as revealed by thin-layer chromatography (TLC) analysis, and the  $^1\text{H}$  NMR signals of the new product's aromatic protons were shifted upfield (Fig. S4†). Further NMR and MS analyses confirmed the new product as **R1-OH** (Scheme 2, Fig. S5 and S6†). Then, the emission spectrum of purified **R1-OH** was compared with probe **R1**, **R1** +  $\text{H}_2\text{O}_2$  and **R1** +  $\text{ClO}^-$  in EtOH/ $\text{H}_2\text{O}$  (4 : 1, v : v). As shown in Fig. 1b, the emission peaks of **R1-OH**, **R1** and **R1** +  $\text{H}_2\text{O}_2$  were mainly in the blue-cyan colour region, while that of **R1** +  $\text{ClO}^-$  was in the green-yellow region.<sup>14</sup> In addition, the titration of **R1** solution with  $\text{H}_2\text{O}_2$  only resulted in a  $\sim 4$  nm blue shift of the fluorescence emission at  $\sim 481$  nm (Fig. S7†), which was not large enough to induce significant emission colour changes. That is to say, despite the fact that  $\text{H}_2\text{O}_2$  was able to oxidize **R1** into **R1-OH**, the emission spectrum of the oxidized product remained in the same blue-cyan region as **R1**, while the addition of  $\text{ClO}^-$  resulted in different reaction products with vivid emission colour changes. Fluorescence spectroscopic measurements revealed that the addition of  $\text{ClO}^-$  to **R1** solution resulted in almost complete fluorescence quenching at  $\sim 481$  nm and the development of a new emission peak at  $\sim 532$  nm (Fig. 1b). Therefore, the ratio of fluo-

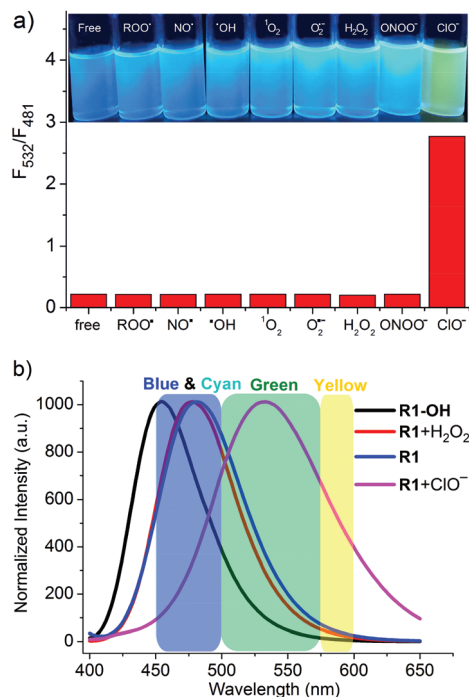
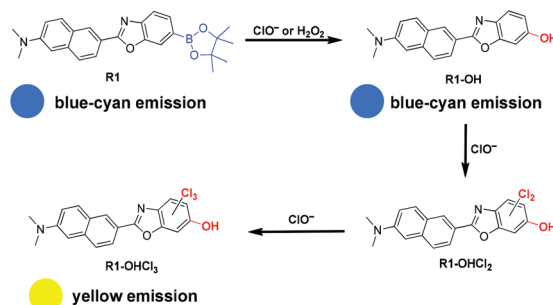


**Fig. 1** Selectivity of **R1** toward  $\text{ClO}^-$  in EtOH/ $\text{H}_2\text{O}$  (4 : 1, v : v). (a) Fluorescence intensity ratio of **R1** (1  $\mu\text{M}$ ) at  $F_{532}/F_{481}$  after the addition of 60 equiv. of various ROS species. Inset: a photograph showing the fluorescence change of **R1** (10  $\mu\text{M}$ ) upon the addition of 60 equiv. of various ROS species in EtOH/ $\text{H}_2\text{O}$  (4 : 1, v : v) under a portable UV lamp irradiation; (b) normalized emission spectra of purified **R1-OH**, **R1** +  $\text{H}_2\text{O}_2$  (60 equiv.), **R1** and **R1** +  $\text{ClO}^-$  (60 equiv.) in EtOH/ $\text{H}_2\text{O}$  (4 : 1, v : v). The colour boxes indicate the spectral range of the corresponding colour.



**Scheme 2** Proposed reaction mechanisms of **R1** upon the addition of  $\text{H}_2\text{O}_2$  and  $\text{ClO}^-$ . Note, chlorination reaction could also occur at the naphthalene ring.

rescence intensities at 532 and 481 nm can be used as a ratiometric reporting signal for the quantitative assessment of the specificity of **R1**. As shown in Fig. 1a, the  $F_{532}/F_{481}$  value was more than ten times higher for  $\text{ClO}^-$  than that for all the other ROS including  $\text{H}_2\text{O}_2$ . These results demonstrated the high selectivity of **R1** for  $\text{ClO}^-$  detection.

The unexpected selectivity of **R1** toward  $\text{ClO}^-$  urged us to investigate the reaction mechanisms between **R1** and  $\text{ClO}^-$ . Therefore, the titration of **R1** solution with  $\text{ClO}^-$  was per-

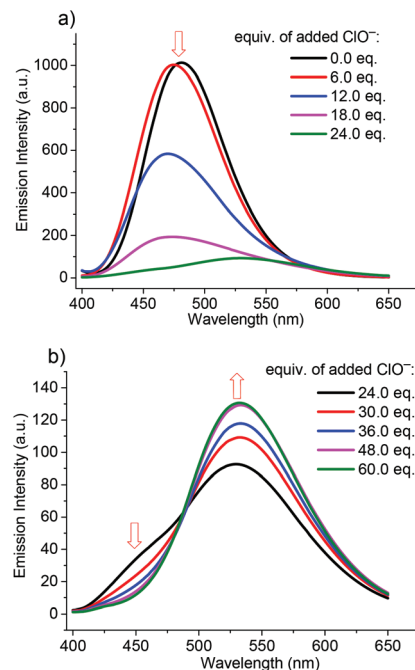


**Fig. 2** Fluorescence titration profile of **R1** (1  $\mu\text{M}$ ) with an increasing amount of  $\text{ClO}^-$  (0–60 equiv.) in  $\text{EtOH}/\text{H}_2\text{O}$  (4 : 1, v : v). (a) 0–24 equiv. of  $\text{ClO}^-$ ; (b) 24–60 equiv. of  $\text{ClO}^-$ .  $\lambda_{\text{ex}} = 370 \text{ nm}$ .

formed using a fluorescence spectrophotometer. Interestingly, two sets of reaction processes were observed. As shown in Fig. 2, the addition of 0–24 equiv. of  $\text{ClO}^-$  to **R1** solution resulted in a  $\sim 10 \text{ nm}$  blue shift and then quenching of the fluorescence emission at  $\sim 481 \text{ nm}$ , whereas further addition of 24–60 equiv. of  $\text{ClO}^-$  led to the development of a new emission peak at  $\sim 532 \text{ nm}$ . For the second interaction process, the distinctive isoemissive point at  $\sim 489 \text{ nm}$  indicated the formation of new species during the second reaction process. Based on the fluorescence titration data, the detection limit of probe **R1** for  $\text{ClO}^-$  was then determined to be  $6.4 \text{ nM}$  based on  $3\sigma/s$ , where  $\sigma$  is the standard deviation of 10 blank measurements and  $s$  is the slope of  $F_{532}/F_{481}$  as a function of  $\text{ClO}^-$  concentration (Fig. S8 and S9<sup>†</sup>). Similarly, multi-step reactions were also observed during the titration of **R1** with  $\text{ClO}^-$  using a UV-visible spectrophotometer (Fig. S10<sup>†</sup>). We noticed that the reaction of **R1** with 6 equiv. of  $\text{ClO}^-$  or 60 equiv. of  $\text{H}_2\text{O}_2$  resulted in almost identical blue shifts ( $\sim 6 \text{ nm}$  for  $\text{ClO}^-$  and  $\sim 4 \text{ nm}$  for  $\text{H}_2\text{O}_2$ ) in the fluorescence emission spectra, indicating the generation of the same product, that is **R1-OH**. Moreover, the addition of  $\text{ClO}^-$  to the purified **R1-OH** generated a similar emission peak to **R1** +  $\text{ClO}^-$  (Fig. S11<sup>†</sup>). These results suggested that **R1-OH** should be the final product of the reaction between **R1** and  $\text{H}_2\text{O}_2$ , but an intermediate for the reaction between **R1** and  $\text{ClO}^-$  (the first reaction step). This conclusion was further supported by the NMR titration data (*vide infra*).

To elucidate the final reaction products of **R1** +  $\text{ClO}^-$ , the reaction was carefully investigated by NMR and MS. As discussed above, since we have determined **R1-OH** to be an inter-

mediate for the reaction between **R1** and  $\text{ClO}^-$ , we envisioned that the initial addition of  $\text{ClO}^-$  to the solution of **R1** might cause boronate oxidation similar to that by  $\text{H}_2\text{O}_2$ . Indeed, the boronate oxidation reaction was observed during the initial titration of **R1** in  $\text{DMSO-d}_6$  with  $\text{ClO}^-$ , as the boronate protons at  $\sim 1.32 \text{ ppm}$  fully disappeared and the peak at  $\sim 3.07 \text{ ppm}$  assigned to the  $-\text{N}-(\text{CH}_3)_2$  protons of **R1** was shifted upfield to  $\sim 3.06 \text{ ppm}$  upon the addition of 1 equiv. of  $\text{ClO}^-$  (Fig. 3). Upon the successive addition of 2–4 equiv. of  $\text{ClO}^-$ , two new peaks assigned to  $-\text{N}-(\text{CH}_3)_2$  were then developed at  $\sim 3.05$  and  $\sim 3.02 \text{ ppm}$ , accompanied by the disappearance of the peak at  $3.06 \text{ ppm}$  (Fig. 3), indicating that two new products (**R1-OHCl<sub>2</sub>** and **R1-OHCl<sub>3</sub>**, *vide infra*) were generated after the boronate oxidation reaction. Complicated proton signals in the low-field region of the  $^1\text{H}$  NMR spectra were observed upon the addition of  $\text{ClO}^-$  (Fig. S12<sup>†</sup>), indicating a mixture of new products. Further addition of more than 4 equiv. of  $\text{ClO}^-$  resulted in precipitation in the NMR tube and no further NMR data could be obtained. Luckily, we successfully isolated the final main reaction product of **R1** +  $\text{ClO}^-$ , and discovered only 6 aromatic protons from its  $^1\text{H}$  NMR data (Fig. S13<sup>†</sup>). It was possible that the addition of  $\text{ClO}^-$  to the solution of **R1** resulted in chlorination reaction at the aromatic rings. This conclusion was further supported by the MS data. The MS data of **R1** after the reaction with different equiv. of  $\text{ClO}^-$  showed that two main products were formed (*i.e.*, **R1-OHCl<sub>2</sub>** ( $m/z$ : 370.9,  $[\text{M}-\text{H}]^-$ ) and **R1-OHCl<sub>3</sub>** ( $m/z$ : 404.9,  $[\text{M}-\text{H}]^-$ )). Moreover, the percentage of **R1-OHCl<sub>3</sub>** increased along with the addition of more equiv. of  $\text{ClO}^-$  (Scheme 2, Fig. S14<sup>†</sup>). The above results suggested that the addition of  $\text{ClO}^-$  first played the same role as  $\text{H}_2\text{O}_2$  to oxidize **R1** into **R1-OH**, and then chlorinated **R1-OH** to **R1-OHCl<sub>2</sub>** and eventually **R1-OHCl<sub>3</sub>** (Scheme 2).

To test if the arylboronate of **R1** could function as a “lock” to eliminate pH induced signal fluctuations, a comparison study between **R1** and **R1-OH** was carried out. Interestingly, though **R1-OH** does not have the arylboronate group, it can be selectively chlorinated by  $\text{ClO}^-$  to produce the yellow emissive product. Therefore, **R1-OH** could also be used as a highly specific fluorescent probe for  $\text{ClO}^-$  detection (Fig. S15<sup>†</sup>). However, the fluorescence of **R1-OH** was greatly influenced by pH, which was possibly due to the protonation/deprotonation

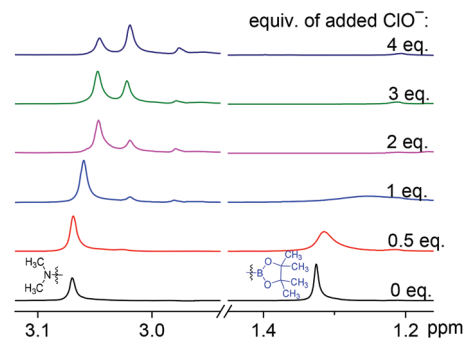


**Fig. 3** High-field region of the  $^1\text{H}$  NMR spectra of **R1** (20 mM) in  $\text{DMSO-d}_6$  upon successive addition of  $\text{ClO}^-$  solution.

reaction at the phenol group of **R1-OH** (Fig. S16<sup>†</sup>). In contrast, **R1** was able to detect  $\text{ClO}^-$  robustly in a wide pH range from 4.5 to 9.0 (Fig. S17<sup>†</sup>). Thus, the arylboronate unit in **R1** functioned as a “lock” for effectively preventing the pH induced fluorescence fluctuation of **R1**.

The proposed multistep reaction mechanism drew our attention into an important issue in designing fluorescent probes, which is the response speed. It is well known that reaction based fluorescent probes usually suffer from the slow response speed, which limits their sensing performance. For probe **R1**, only about 2 min were required to complete the reaction at room temperature, which fully met the sensing requirements (Fig. S18<sup>†</sup>). In addition to its merits, such as fast response speed, high sensitivity, selectivity and pH tolerance for  $\text{ClO}^-$  detection, **R1** was highly photostable. The photostable test showed that the fluorescence intensity of **R1** at 481 nm did not show obvious decay upon continuous irradiation under 365 nm UV light for 4 h (Fig. S19<sup>†</sup>). These results indicated that **R1** was a promising fluorescent probe for  $\text{ClO}^-$  detection.

## Conclusions

In conclusion, a ratiometric fluorescent probe **R1** was developed for specific  $\text{ClO}^-$  detection. Detailed mechanistic studies revealed that **R1** reacted with  $\text{ClO}^-$  through an oxidation to chlorination mechanism. Moreover, the arylboronate moiety in **R1** acted as a “lock” to prevent the pH influence on its  $\text{ClO}^-$  sensing behavior. **R1** was not only highly stable and robust but also exhibited high sensitivity and selectivity for  $\text{ClO}^-$ . This work unravelled the mechanism of the specific response of an arylboronate contained fluorophore to  $\text{ClO}^-$  over other ROS including  $\text{H}_2\text{O}_2$ , and demonstrated an effective strategy for designing highly robust probes by introducing a “lock” moiety.

## Acknowledgements

We thank the National Natural Science Foundation of China (no. 21405081), the Natural Science Foundation of Jiangsu Province (no. BK20140593 and no. BK20130561), the 973 Program (no. 2015CB659400), the Priority Academic Program Development of Jiangsu Higher Education Institutions (PAPD), the Shuangchuang Program of Jiangsu Province, the Six Talents Summit Program of Jiangsu Province, Open Funds of the State Key Laboratory for Chemo/Biosensing and Chemometrics (2014002), Open Funds of the State Key Laboratory of Electroanalytical Chemistry (SKLEAC201501), Open Funds of the State Key Laboratory of Analytical Chemistry for Life Science (SKLACLS1704), the Fundamental Research Funds for the Central Universities (KYZ201750), and the Thousand Talents Program for Young Researchers for financial support. We thank Professor Yong Liang, Professor Bingling Li, Professor Yongshu Xie, Dr Jing Liu, and Dr Shiliang Tian for helpful discussions.

## Notes and references

- (a) A. R. Lippert, G. C. Van de Bittner and C. J. Chang, *Acc. Chem. Res.*, 2011, **44**, 793–804; (b) T. Finkel and N. J. Holbrook, *Nature*, 2000, **408**, 239–247; (c) F. Wen, Y. Dong, L. Feng, S. Wang, S. Zhang and X. Zhang, *Anal. Chem.*, 2011, **83**, 1193–1196; (d) Y. Huang, F. Yu, J. Wang and L. Chen, *Anal. Chem.*, 2016, **88**, 4122–4129; (e) L.-Y. Wang, H.-Y. Su, X. Wang, Y. Zhou and S.-J. Yang, *Chin. J. Anal. Chem.*, 2015, **43**, 1870–1875.
- (a) Z. M. Prokopowicz, F. Arce, R. Biedron, C. L.-L. Chiang, M. Ciszek, D. R. Katz, M. Nowakowska, S. Zapotoczny, J. Marcinkiewicz and B. M. Chain, *J. Immunol.*, 2010, **184**, 824–835; (b) Y. W. Yap, M. Whiteman and N. S. Cheung, *Cell Signalling*, 2007, **19**, 219–228.
- (a) L. M. Zheng, B. Nukuna, M. L. Brennan, M. J. Sun, M. Goormastic, M. Settle, D. Schmitt, X. M. Fu, L. Thomson, P. L. Fox, H. Ischiropoulos, J. D. Smith, M. Kinter and S. L. Hazen, *J. Clin. Invest.*, 2004, **114**, 529–541; (b) L. J. Hazell, L. Arnold, D. Flowers, G. Waeg, E. Malle and R. Stocker, *J. Clin. Invest.*, 1996, **97**, 1535–1544.
- E. Malle, T. Buch and H.-J. Grone, *Kidney Int.*, 2003, **64**, 1956–1967.
- J. K. Andersen, *Nat. Med.*, 2004, **10**, S18–S25.
- (a) N. Güngör, A. M. Knaapen, A. Munnia, M. Peluso, G. R. Haenen, R. K. Chiu, R. W. L. Godschalk and F. J. van Schooten, *Mutagenesis*, 2010, **25**, 149–154; (b) S. A. Weitzman and L. I. Gordon, *Blood*, 1990, **76**, 655–663.
- (a) W. Chyan, D. Y. Zhang, S. J. Lippard and R. J. Radford, *Proc. Natl. Acad. Sci. U. S. A.*, 2014, **111**, 143–148; (b) S. Bhuniya, S. Maiti, E.-J. Kim, H. Lee, J. L. Sessler, K. S. Hong and J. S. Kim, *Angew. Chem., Int. Ed.*, 2014, **53**, 4469–4474; (c) Y. Ding, W.-H. Zhu and Y. Xie, *Chem. Rev.*, 2017, **117**, 2203–2256; (d) X. Chen, F. Wang, J. Y. Hyun, T. Wei, J. Qiang, X. Ren, I. Shin and J. Yoon, *Chem. Soc. Rev.*, 2016, **45**, 2976–3016; (e) C. M. Lemon, E. Karnas, X. Han, O. T. Bruns, T. J. Kempa, D. Fukumura, M. G. Bawendi, R. K. Jain, D. G. Duda and D. G. Nocera, *J. Am. Chem. Soc.*, 2015, **137**, 9832–9842; (f) X. Qian and Z. Xu, *Chem. Soc. Rev.*, 2015, **44**, 4487–4493; (g) Y. Ding, L. Shi and H. Wei, *Chem. Sci.*, 2015, **6**, 6361–6366; (h) Y. Ni and J. Wu, *Org. Biomol. Chem.*, 2014, **12**, 3774–3791; (i) Y. Yang, Q. Zhao, W. Feng and F. Li, *Chem. Rev.*, 2013, **113**, 192–270; (j) X. Wu, X. Sun, Z. Guo, J. Tang, Y. Shen, T. D. James, H. Tian and W. Zhu, *J. Am. Chem. Soc.*, 2014, **136**, 3579–3588; (k) X. Li, X. Gao, W. Shi and H. Ma, *Chem. Rev.*, 2013, **114**, 590–659; (l) D. Zamora-Olivares, T. S. Kaoud, J. Jose, A. Ellington, K. N. Dalby and E. V. Anslyn, *Angew. Chem., Int. Ed.*, 2014, **53**, 14064–14068; (m) Y. Wen, K. Liu, H. Yang, Y. Li, H. Lan, Y. Liu, X. Zhang and T. Yi, *Anal. Chem.*, 2014, **86**, 9970–9976; (n) W. Zhang, P. Li, F. Yang, X. Hu, C. Sun, W. Zhang, D. Chen and B. Tang, *J. Am. Chem. Soc.*, 2013, **135**, 14956–14959; (o) G.-Q. Yu, Z.-L. Yuan, J. Yang, Q. Wu, Q.-H. Hu, M.-Q. Zhang, B. Jiang and G. Wei, *Chin. J. Anal. Chem.*, 2016, **44**, 1495–1503.

- 8 J. Ballesta Claver, M. C. Valencia Mirón and L. F. Capitán-Vallvey, *Anal. Chim. Acta*, 2004, **522**, 267–273.
- 9 L. Lu, J. Zhang and X. Yang, *Sens. Actuators, B*, 2013, **184**, 189–195.
- 10 O. Ordeig, R. Mas, J. Gonzalo, F. J. DelCampo, F. J. Muñoz and C. de Haro, *Electroanalysis*, 2005, **17**, 1641–1648.
- 11 (a) Y. Koide, Y. Urano, K. Hanaoka, T. Terai and T. Nagano, *J. Am. Chem. Soc.*, 2011, **133**, 5680–5682; (b) J. J. Hu, N.-K. Wong, M.-Y. Lu, X. Chen, S. Ye, A. Q. Zhao, P. Gao, R. Yi-Tsun Kao, J. Shen and D. Yang, *Chem. Sci.*, 2016, **7**, 2094–2099; (c) Y. Yue, F. Huo, C. Yin, J. O. Escobedo and R. M. Strongin, *Analyst*, 2016, **141**, 1859–1873; (d) H. Zhu, J. Fan, J. Wang, H. Mu and X. Peng, *J. Am. Chem. Soc.*, 2014, **136**, 12820–12823; (e) Q. Xu, K.-A. Lee, S. Lee, K. M. Lee, W.-J. Lee and J. Yoon, *J. Am. Chem. Soc.*, 2013, **135**, 9944–9949; (f) X. Wu, Z. Li, L. Yang, J. Han and S. Han, *Chem. Sci.*, 2013, **4**, 460–467; (g) S. T. Manjare, J. Kim, Y. Lee and D. G. Churchill, *Org. Lett.*, 2014, **16**, 520–523; (h) M. Sun, H. Yu, H. Zhu, F. Ma, S. Zhang, D. Huang and S. Wang, *Anal. Chem.*, 2014, **86**, 671–677.
- 12 (a) M. Ren, B. Deng, K. Zhou, X. Kong, J.-Y. Wang and W. Lin, *Anal. Chem.*, 2017, **89**, 552–555; (b) L. Yuan, W. Lin, Y. Xie, B. Chen and S. Zhu, *J. Am. Chem. Soc.*, 2011, **134**, 1305–1315; (c) B. C. Dickinson and C. J. Chang, *J. Am. Chem. Soc.*, 2008, **130**, 9638–9639; (d) G. Li, D. Zhu, Q. Liu, L. Xue and H. Jiang, *Org. Lett.*, 2013, **15**, 924–927; (e) J. Xu, Y. Zhang, H. Yu, X. Gao and S. Shao, *Anal. Chem.*, 2016, **88**, 1455–1461.
- 13 A. Sikora, J. Zielonka, M. Lopez, J. Joseph and B. Kalyanaraman, *Free Radicals Biol. Med.*, 2009, **47**, 1401–1407.
- 14 It was also surprising to find that the maximum emission peak of **R1-OH** was obviously blue shifted (481 to 454 nm) relative to the unpurified **R1** + H<sub>2</sub>O<sub>2</sub> system. This may be due to the presence of complicated ingredients in the solution of **R1** + H<sub>2</sub>O<sub>2</sub> than the pure **R1-OH**.